

# Carbon Nanotube Field-Effect Transistor for DNA Sensing

CHU T. XUAN,<sup>1</sup> NGUYEN T. THUY,<sup>1,2</sup> TRAN T. LUYEN,<sup>1</sup>  
TRAN T.T. HUYEN,<sup>1</sup> and MAI A. TUAN<sup>1,3,4</sup>

1.—International Training Institute for Materials Science (ITIMS), Hanoi University of Science and Technology (HUST), No. 1, Dai Co Viet Road, Hai Ba Trung District, Hanoi, Vietnam. 2.—Electric Power University (EPU), No. 235, Hoang Quoc Viet Road, Hanoi, Vietnam. 3.—e-mail: mtuan@itims.edu.vn. 4.—e-mail: tuan.maianh@hust.edu.vn

A field-effect transistor (FET) using carbon nanotubes (CNTs) as the conducting channel (CNTFET) has been developed, designed such that the CNT conducting channel (15  $\mu\text{m}$  long, 700  $\mu\text{m}$  wide) is directly exposed to medium containing target deoxyribonucleic acid (DNA). The CNTFET operates at high ON-current of 1.91  $\mu\text{A}$ , ON/OFF-current ratio of  $1.2 \times 10^5$ , conductance of 4.3  $\mu\text{S}$ , and leakage current of 16.4 pA. We present initial trials showing the response of the CNTFET to injection of target DNA into aqueous medium.

**Key words:** Field-effect transistor, CNTFET, DNA sensor

## INTRODUCTION

Since the first paper on ion-sensitive field-effect transistors (ISFETs) in the 1970s,<sup>1</sup> thousands of papers have appeared in literature, discussing technological developments for various applications. The ISFET is a metal–oxide–semiconductor FET where the metal gate is replaced by the combination of an ion-selective membrane and a reference electrode that is directly exposed to an electrolyte solution. The principle of operation of such a device has been well discussed in numerous works.<sup>2–4</sup>

Due to their low fabrication cost and reduced size, ISFETs are often used in chemically based lab-on-chip systems. For deoxyribonucleic acid (DNA) detection, in particular, it is necessary to immobilize a single strand of oligonucleotide (probe) onto the ion-selective membrane. In the measurement medium, this probe specifically binds to target DNA, altering the source–drain current.

Using conventional fabrication methods, the conducting channel of the ISFET can be obtained by thermal diffusion or ion implantation of a predetermined concentration of *n*- or *p*-type dopant. Because of their exceptional electrical, thermal, and

mechanical properties,<sup>5–7</sup> carbon nanotubes (CNTs) have also been examined for formation of the conducting channel of FET structures.<sup>8,9</sup> CNTs are typically coated on the region between the source and drain of the FET structure, where the gate can be either on top (front) or underneath the substrate.

In back-gate CNTFETs, the contact resistance is normally greater than 1 M $\Omega$ , leading to low transconductance ( $g_m = dI/dV_G$ ) of about  $10^{-9}$  A/V. In addition, the thickness of the conducting layer of the gate is usually greater than 100 nm, requiring higher gate voltage for transistor operation.<sup>10</sup> For decades, efforts have been made to improve these issues.

The front-gate CNTFET configuration requires a small controlling voltage for device operation. However, the fabrication process is more complicated, requiring a high-end cleanroom. Since the conducting channel is buried underneath the gate oxide, it is also difficult to immobilize species for biological recognition.<sup>9,11</sup>

With application in DNA sensors in mind, in this work, CNTs were deposited on top of the field oxide layer, creating the conducting channel of the FET (Fig. 1), while the contact was prepared on the backside of the substrate. This type of structure was recently reported in Ref. 12. We present herein the results of trial experiments conducted to assess the possible application of such CNTFETs for sensing of DNA in aqueous solution.



Fig. 1. FET-based DNA sensor.

## EXPERIMENTAL PROCEDURES

### Chemicals and Apparatus

Single-walled CNTs (95%,  $R < 2$  nm,  $5 \mu\text{m}$  to  $15 \mu\text{m}$  in length) were purchased from Shenzhen Nanotech Port Co. Ltd. Nitric acid (65%), fuming  $\text{H}_2\text{SO}_4$  (98%), chloric acid, fluoric acid (1%), 3-aminopropyltriethoxysilane (APTES),  $N,N$ -dimethylformamide (DMF), acetone, methanol, and isopropanol were purchased from Sigma-Aldrich. The chemicals were of analytical grade. A (100)-oriented, 4-inch,  $300\text{-}\mu\text{m}$ -thick silicon wafer with resistivity of  $0.01 \Omega \text{ cm}$  was obtained from Philips.

Influenza virus DNA, as advised by the National Institute of Hygiene and Epidemiology of Vietnam, was provided by Invitrogen; its sequence is presented in Table I. The FET mask was designed using CleWin software. The length of the channel was  $15 \mu\text{m}$ , and its width was  $700 \mu\text{m}$ .

### CNTFET Fabrication

The fabrication process for the CNTFET was conducted at the Hanoi University of Science and Technology. A  $100\text{-nm}$   $\text{SiO}_2$  layer was thermally grown on a clean silicon substrate. Then, the  $\text{SiO}_2$  surface was functionalized by formation of silanol  $\text{SiOH}$  and  $-\text{OH}$  functional groups,<sup>13</sup> followed by deposition of CNTs dispersed in DMF<sup>14</sup> on the channel region of the FETs by a dropping technique. A metal mask was required to protect the other areas of the device. Residual DMF in the membrane was evacuated by heat treatment at  $200^\circ\text{C}$  for 120 min. Source and drain contacts were formed by a conventional photolithography and liftoff process using a contact photoresist mask, etching the metal around the mask to leave patterns in the form of the mask design. The back gate of the CNTFET was created by thermal evaporation of aluminum. For surface stabilization, after evaporation in a vacuum chamber, the Al membrane was annealed in  $\text{N}_2$  at  $450^\circ\text{C}$  for 30 min.

### Measurement Setup

All characteristics of the CNTFETs were examined and evaluated using an HP4155C precision

Table I. DNA sequences

Sequence	Description
5'-AT CAC CGA CCC GGA GAG GGA C-3'	Probe
3'-TA GTG GCT GGG CCT CTC CCT G-5'	Target

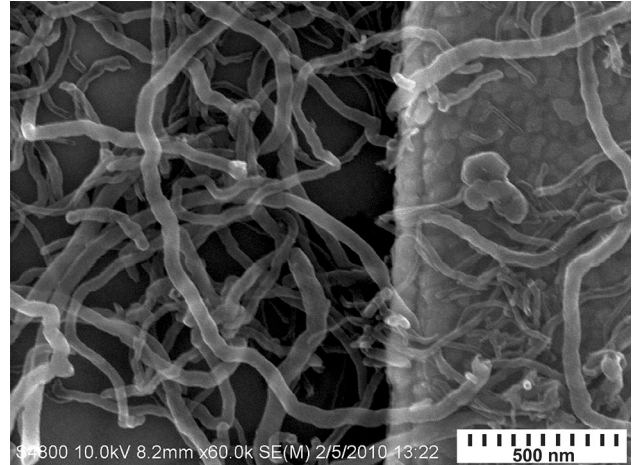


Fig. 2. Micrograph of CNT surface channel.

semiconductor parameter analyzer at room temperature. The source of the CNTFETs was commonly grounded with the back side, i.e.,  $V_S = 0$ . The  $I_D$ - $V_{DS}$  characteristic of the CNTFETs was tested at direct-current (DC) drain voltage of  $V_{DS} = 0$  V to  $10$  V in steps of  $-0.04$  V and gate voltage of  $V_{GS} = -10$  V to  $4$  V in steps of  $2$  V. To determine the transfer characteristic ( $I_D$ - $V_{GS}$ ), a gate voltage of  $10$  V to  $-10$  V (in steps of  $0.1$  V) was applied, with the drain voltage  $V_{DS}$  set from  $-0.5$  V to  $-1.5$  V in steps of  $-0.5$  V.

### DNA Immobilization and Signal Readout

DNA was immobilized onto the CNT gate of the transistor by physical adsorption. The surface of the CNTFET was treated by soaking in phosphate-buffered saline (PBS) then washed with deionized (DI) water five times. After that, the transistors were incubated in  $10 \mu\text{M}$  of DNA probe solution for 3 h, followed by rinsing with PBS and DI water five times to remove weakly bound DNA molecules. Hybridization experiments were performed by immersing the DNA chip in  $1 \text{ pM}$  solution of target DNA dissolved in  $30 \text{ mM}$  PBS.  $I_D$  was measured at constant bias voltage ( $V_{DS} = -0.5$  V) while sweeping  $V_{GS}$  from  $-10$  V to  $+10$  V in steps of  $0.1$  V.

## RESULTS AND DISCUSSION

### Micrograph of CNT Surface Channel

The scanning electron microscopy image in Fig. 2 shows the morphology of the channel surface functionalized with the modified CNTs. The CNT

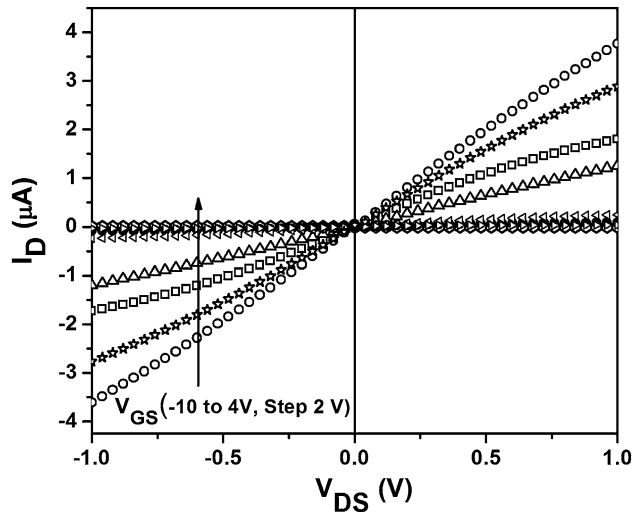


Fig. 3. Ohmic contact characteristics of the FET.

network was distributed and covered by the source and drain contacts, as in the designed mask.

### CNTFET Characteristics

The contact between the metal part of the source/drain and the semiconductor was made ohmic with the lowest possible contact resistance during the FET fabrication. According to the results in Fig. 3, the  $I_D$ - $V_{DS}$  relation of the CNTFETs was linear in the  $V_{DS}$  range from  $-1$  V to  $1$  V with resistance of  $380$  k $\Omega$ . This value is higher than reported in Ref. 15 ( $50$  k $\Omega$ ), but much lower than those obtained in the work of Tans<sup>8</sup> ( $1$  M $\Omega$ ). In this work, the low contact resistance was found not only at the interface between the CNTs and metal electrode, but also within the CNT network.

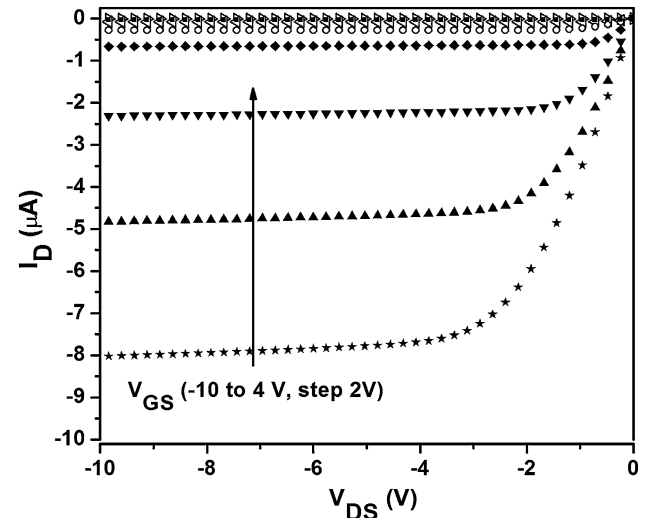
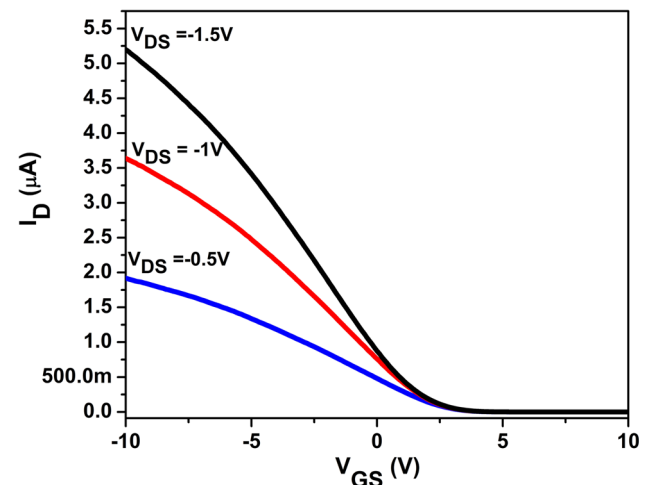
### $I_D$ - $V_{DS}$ Characteristic

Figure 4 illustrates the  $I_D$ - $V_{DS}$  characteristic as a function of applied gate voltage. The drain current,  $I_D$ , connects the source and drain of the CNTFET ( $p$ -type) and exists even at  $V_{GS} = 0$  V. When  $V_{GS} > 0$  V, the device was in OFF-state.

In contrast, when  $V_{GS} < 0$  V, the device was in ON-state. The  $I_D$ - $V_{DS}$  characteristics were the same as those of a  $p$ -type FET, which is well described in literature.

### Transfer $I_D$ - $V_{GS}$ Characteristic

The CNTFET functions by movement of holes as majority carriers. For a  $p$ -type FET, in the forward-bias region, the applied gate and drain voltage must be negative. As shown in Fig. 5, changing the gate voltage led to a change in the density of holes in the channel (where the CNTs are); in turn, the channel resistance and current density also changed. The  $I_D$ - $V_{GS}$  transfer curve was observed at each stepped value of  $V_{DS}$  ( $-0.5$  V,  $-1.0$  V, and  $-1.5$  V).

Fig. 4.  $I_D$ - $V_{DS}$  characteristics versus applied gate voltage for the FET.Fig. 5. Transfer  $I_D$ - $V_{GS}$  characteristics of the FET.

### Threshold Voltage

The threshold voltage  $V_T$  is the value at which the device switches between ON- and OFF-state. As presented in Fig. 6, when the gate voltage was greater than  $2.6$   $V_{DC}$ , there was almost no  $I_D$  current, so the device was in OFF-state.

When the gate voltage was slightly below  $2.6$   $V_{DC}$  and shifted toward the negative region, the  $I_D$  current became different from zero and increased quickly because the CNTs changed from insulating to conductive state; therefore, the device was then in ON-state.

### ON/OFF-Current Ratio

Figure 7 presents the  $I_D$ - $V_{GS}$  transfer characteristics of the CNTFETs on a logarithmic scale. The open current, at  $V_{DS} = -0.5$  V and  $V_{GS} = -10$  V, was  $1.91$   $\mu$ A, corresponding to current density of

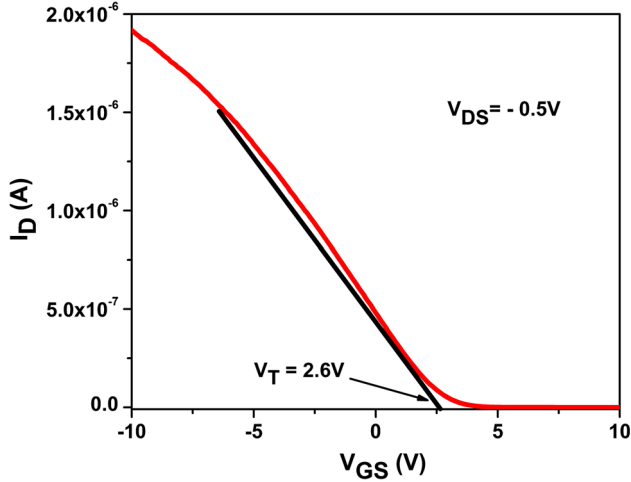


Fig. 6. Threshold voltage of the FET.

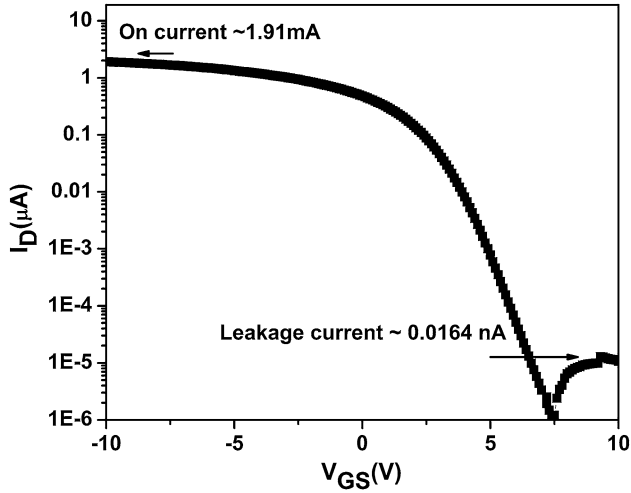


Fig. 7. ON/OFF-current ratio and leakage current of FET.

$0.0027 \mu\text{A}/\mu\text{m}^2$ . Meanwhile, the leakage current was tiny at  $0.0164 \text{ nA}$ . This high ON/OFF-current ratio of  $1.2 \times 10^5$  can be explained by the high density and homogeneity of the CNT network on the APTES-modified Si/SiO<sub>2</sub> surface, being very beneficial for sensor fabrication.

The transconductance of the FET, in the linear region, was calculated as<sup>16</sup>:

$$G_m = \frac{dI_D}{dV_{GS}} = \frac{W}{L} C_{ox} \cdot \mu_{eff} \cdot V_{DS}. \quad (1)$$

From the  $I_D$ - $V_{GS}$  transfer characteristics of the CNTFETs ( $L_1 = 15 \mu\text{m}$ ,  $W = 700 \mu\text{m}$ ) at  $V_{DS} = -0.5 \text{ V}$ , one can plot  $G_m$  versus  $V_{GS}$  (not shown), from which the transconductance,  $G_{max}$ , was calculated to be  $0.22 \mu\text{S}$  in the linear region.

### Conductance

The conductance in the linear region ( $V_{DS} < V_{GS} - V_T$ ) can be expressed as follows<sup>17</sup>:

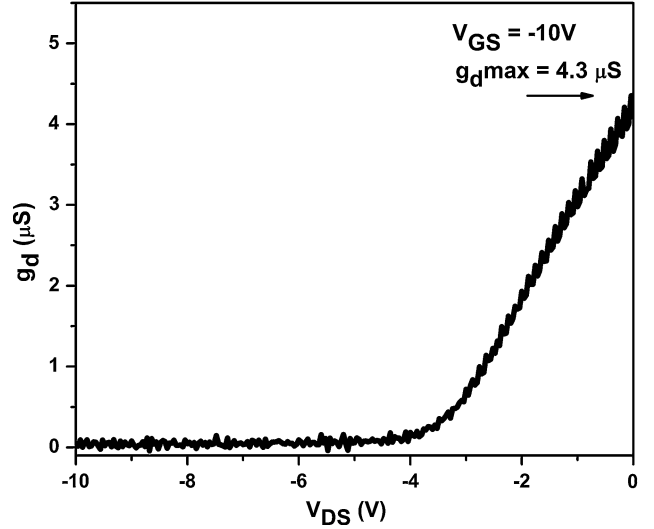


Fig. 8. Conductance of the FET.

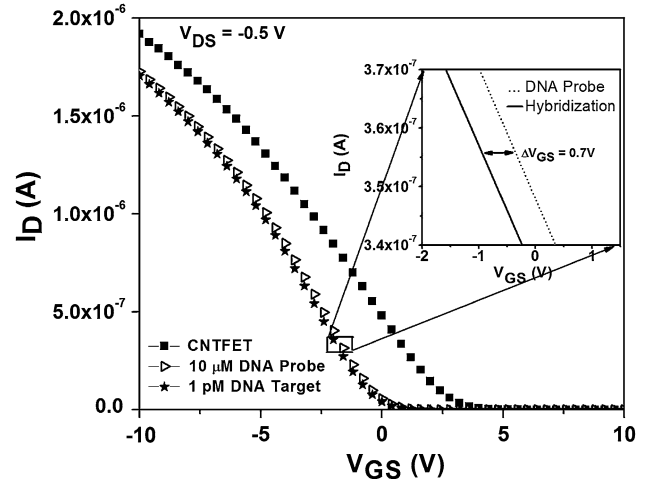


Fig. 9. The drain current decreases on injection of a DNA sequence. The inset shows the voltage shift due to addition of target DNA.

$$g_d = \frac{dI_D}{dV_{DS}} = \frac{W}{L} C_{ox} \times \mu_{eff} \times (V_{GS} - V_T). \quad (2)$$

From the  $I_D$ - $V_{DS}$  output characteristics in the linear region, with  $V_{GS} = -10 \text{ V}$ , one can plot  $g_d = f(V_{DS})$ , as shown in Fig. 8; the maximum conductance was found to be  $4.3 \mu\text{S}$ . The resistance,  $R$ , of the CNTFETs, calculated as the inverse value of the conductance in ON-state, was  $233 \text{ k}\Omega$ .

### DNA Concentration Response

Figure 9 illustrates the transfer characteristics recorded in the case of CNTFETs with no DNA, with DNA probe, and with probe-target hybridization.

Binding of the probe DNA increased the electron concentration, resulting in a reduction of the majority carriers in the channel of the CNTFETs,<sup>16</sup> which leads to a decrease in the drain current  $I_D$ . The



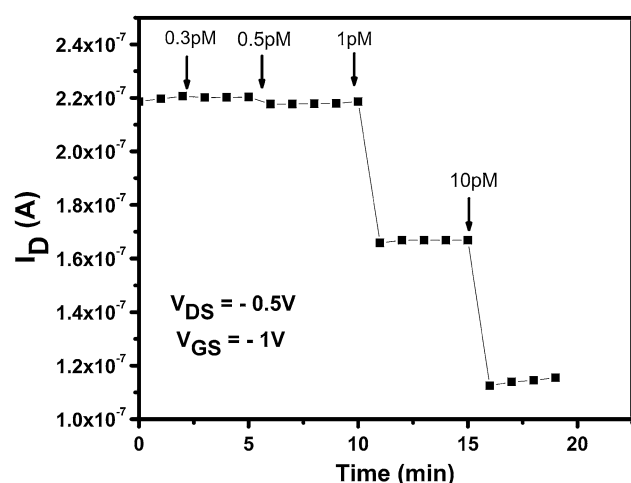


Fig. 10. Response time of DNA sensor.

drain current keeps reducing due to hybridization with increasing concentration of target DNA, based on which it is possible to establish and plot the drain current versus DNA concentration. Figure 9 (inset) also shows the shift of 0.7 V of the gate voltage due to the  $V_{GS}$ - $I_{DS}$  relation.

Figure 10 shows that the CNTFET-based DNA sensor did not respond to target concentrations of 0.3 pM and 0.5 pM, while a net drain current change was observed when 1 pM and 10 pM target was injected into the measurement cell. The response time was less than 1 min in both cases.

## CONCLUSIONS

The CNTFET in this work operates with very small leakage current, high ON/OFF-current ratio, and low threshold voltage. Physical adsorption was used to immobilize probe DNA onto the CNT conducting channel of the transistor. Hybridization between the target DNA and probe changed the conductance of the channel and the current density

of the FETs. Based on the results, it is possible to establish a relationship between the target DNA concentration in solution and the  $I_{DS}$  of the transistor. Initial experiments showed that the CNTFET-based DNA sensor could detect injection of 1 pM target DNA in just under 1 min. Further research should be conducted to investigate possible factors that impact the characteristics of such CNTFET-based DNA sensors.

## ACKNOWLEDGEMENTS

This work was financially supported by the Vietnamese National Foundation for Science and Technology Development (NAFOSTED) under Project Code No. 103.99-2013.58.

## REFERENCES

1. P. Bergveld, *IEEE Trans. Biomed. Eng.* 17, 70 (1970).
2. P. Bergveld, *Sens. Actuators B Chem.* 88, 1 (2003).
3. J. Bausells, J. Carrabina, A. Errachid, and A. Merlos, *Sens. Actuators B Chem.* 57, 56 (1999).
4. L.M. Shepherd, S. Member, and C. Toumazou, *IEEE Trans. Circuits Syst. I Fundam. Theory Appl.* 52, 2614 (2005).
5. S. Iijima and I. Toshinari, *Nature* 363, 03 (1993).
6. V.N. Popov, *Mater. Sci. Eng., R* 43, 61 (2004).
7. S.I. Cha, K.T. Kim, K.H. Lee, C.B. Mo, Y.J. Jeong, and S.H. Hong, *Carbon* 46, 482 (2008).
8. S.J. Tans, A.R.M. Verschueren, and C. Dekker, *Nature* 393, 49 (1998).
9. P. Avouris, *Acc. Chem. Res.* 35, 1026 (2002).
10. R. Martel, T. Schmidt, H.R. Shea, T. Hertel, and P. Avouris, *Appl. Phys. Lett.* 73, 2447 (1998).
11. S.J. Wind, J. Appenzeller, R. Martel, V. Derycke, and P. Avouris, *Appl. Phys. Lett.* 80, 3817 (2002).
12. F. Yuan, Y. Deng, W. Zhou, M. Zhang, and Z. Li, *Nano Res.* 9, 1701 (2016).
13. Y. Han, D. Mayer, A. Offenha, and S. Ingebrandt, *Thin Solid Films* 510, 175 (2006).
14. T.T. Nguyen, S.U. Nguyen, and D.T. Phuong, *Adv. Nat. Sci. Nanosci. Nanotechnol.* 2, 1 (2011).
15. A. Javey, Q. Wang, W. Kim, and H. Dai, *IEEE International Electron Devices Meeting* (2004), pp. 1-4.
16. S.H. Jin, A.E. Islam, T. Kim, J. Kim, M.A. Alam, and J.A. Rogers, *Adv. Funct. Mater.* 22, 2276 (2012).
17. M. Simon and N. Kwok, *Physics of Semiconductor Devices*, 3rd ed. (Hoboken: Wiley-Interscience, 2007).